

Three-body forces and shell structure in calcium isotopes

Jason D. Holt,^{1,2} Takaharu Otsuka,^{3,4} Achim Schwenk,^{5,6} and Toshio Suzuki⁷

¹*Department of Physics and Astronomy, University of Tennessee, Knoxville, TN 37996, USA*

²*Physics Division, Oak Ridge National Laboratory, P.O. Box 2008, Oak Ridge, TN 37831, USA*

³*Department of Physics and Center for Nuclear Study,
University of Tokyo, Hongo, Tokyo 113-0033, Japan*

⁴*National Superconducting Cyclotron Laboratory, Michigan State University, East Lansing, MI, 48824, USA*

⁵*ExtreMe Matter Institute EMMI, GSI Helmholtzzentrum für Schwerionenforschung GmbH, 64291 Darmstadt, Germany*

⁶*Institut für Kernphysik, Technische Universität Darmstadt, 64289 Darmstadt, Germany*

⁷*Department of Physics, Nihon University, Sakurajosui 3, Tokyo 156-8550, Japan*

Understanding and predicting the formation of shell structure from nuclear forces is a central challenge for nuclear physics. While the magic numbers $N = 2, 8, 20$ are generally well understood, $N = 28$ is the first standard magic number that is not reproduced in microscopic theories with two-nucleon forces. In this Letter, we show that three-nucleon forces give rise to repulsive interactions between two valence neutrons that are key to explain ^{48}Ca as a magic nucleus, with a high 2^+ excitation energy and a concentrated magnetic dipole transition strength. The repulsive three-nucleon mechanism improves the agreement with experimental binding energies.

PACS numbers: 21.10.-k, 21.30.-x, 21.60.Cs, 27.40.+z

In nuclei certain configurations of protons and neutrons (nucleons) are observed to be particularly well-bound. These closed-shell or “magic” nuclei form the basis of the nuclear shell model (exact diagonalizations in spaces based on the observed shell structure [1]), which provides a key computational method in nuclear physics. Exploring the formation of shell structure and how these magic configurations evolve with nucleon number towards the drip lines is a frontier in the physics of nuclei, and a microscopic understanding from nuclear forces presents a major challenge for theory.

The theoretical shortcomings in predicting shell structure are particularly evident in the calcium isotopes. While microscopic calculations with well-established two-nucleon (NN) forces reproduce the standard magic numbers $N = 2, 8, 20$, one of the most striking failures is that they do not predict ^{48}Ca as a doubly-magic nucleus when neutrons are added to ^{40}Ca [1, 2], making $N = 28$ the first standard magic number not reproduced in microscopic NN theories. As a result, phenomenological forces have been adjusted to yield a doubly-magic ^{48}Ca [3, 4], and it has been argued these phenomenological adjustments may be largely due to neglected three-nucleon (3N) forces [5]. Recently, we have shown that 3N forces play a decisive role for the oxygen anomaly and can explain why ^{24}O is the heaviest oxygen isotope [6]. In this Letter, we present the first study of the impact of 3N forces on medium-mass nuclei. Our results demonstrate that one- and two-body contributions from 3N forces to valence neutrons, as well as extended valence spaces, are essential to understand shell structure in the calcium isotopes and $N = 28$ as a magic number based on nuclear forces.

Three-nucleon forces were introduced in the pioneering work of Fujita and Miyazawa (FM) [7] and arise because nucleons are finite-mass composite particles that can also

be excited by interacting with other particles. The long-range part of 3N forces is dominated by the FM 3N mechanism, where one nucleon virtually excites a second nucleon to the $\Delta(1232\text{ MeV})$ resonance, which is de-excited by interacting with a third nucleon. Additional long-range and shorter-range 3N interactions are included naturally in chiral effective field theory (EFT) [8], which provides a systematic expansion for nuclear forces. The importance of chiral 3N forces has been well established in light nuclei with $A = N + Z \lesssim 12$ [9].

We derive the interactions among valence neutrons following two approaches. First, we use low-momentum interactions $V_{\text{low } k}$ with smooth cutoffs [10] obtained by evolving a chiral N^3LO NN potential [11] to lower resolution with $\Lambda = 2.0\text{ fm}^{-1}$. The two-body interactions in the pf and $pf g_{9/2}$ shell are calculated to third order in many-body perturbation theory (MBPT) following Refs. [12, 13] in a space of 13 major shells. We use a harmonic oscillator basis with $\hbar\omega = 11.48\text{ MeV}$, appropriate for the calcium isotopes. Our results are converged for intermediate-state excitations to $18\hbar\omega$. Second, we take a standard G -matrix that has been used as a starting point in many nuclear-structure calculations [13]. This G matrix is based on the Bonn C NN potential and includes many-body contributions to third order, but with intermediate-state excitations to $2\hbar\omega$ (and calculated for $\hbar\omega = 10\text{ MeV}$). Although the G -matrix calculation should be improved by extending the intermediate states, this two-body interaction has been used as standard starting point for shell-model studies, and gives us a baseline to investigate changes due to three-body forces. A detailed study of the cutoff dependence, which provides a measure of the theoretical uncertainty, is left to future work.

To study the validity of the MBPT approach, we

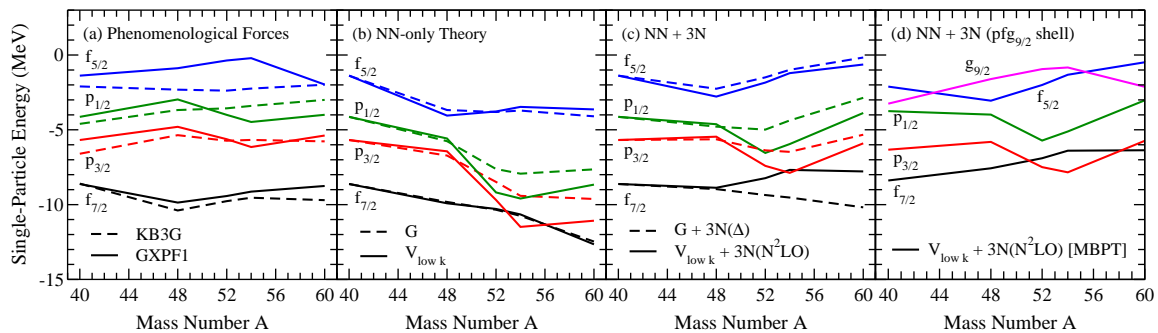


FIG. 1. Neutron SPEs relative to the ^{40}Ca energy as a function of mass number A . (a) SPEs obtained from phenomenological models KB3G [3] and GXPF1 [4]. (b) NN-only theory: SPEs calculated from a G -matrix and low-momentum interactions $V_{\text{low } k}$. (c) SPEs including contributions from 3N forces due to Δ excitations, $3\text{N}(\Delta)$, and chiral EFT 3N interactions at N^2LO , $3\text{N}(\text{N}^2\text{LO})$ [20]. The results in panels (b) and (c) start from the empirical GXPF1 SPEs in ^{41}Ca . (d) SPEs in the $pf g_{9/2}$ shell calculated from $V_{\text{low } k}$ and $3\text{N}(\text{N}^2\text{LO})$ forces, where the starting SPEs in ^{41}Ca are calculated consistently in many-body perturbation theory [MBPT] and include one-body 3N contributions.

have carried out coupled-cluster (CC) calculations for the ground-state energies of $^{40,48,52,54}\text{Ca}$ at the Λ -CCSD(T) level [14], based on the same $V_{\text{low } k}$ interaction and basis space. We have verified that the CC energies are converged in these spaces. Using particle-attached (to ^{40}Ca) CC energies as single-particle energies (SPEs), the MBPT results agree within a few percent with CC theory (relative to ^{40}Ca): -159.3 MeV (MBPT) vs. -155.0 MeV (CC) for ^{48}Ca ; -230.7 MeV vs. -235.9 MeV for ^{52}Ca ; and -259.1 MeV vs. -268.6 MeV for ^{54}Ca . This shows that MBPT can be comparable to CC theory for $V_{\text{low } k}$ interactions, but also highlights the important role of SPEs.

To understand shell structure in the calcium isotopes, we show in Fig. 1 the change of the SPEs of the neutron orbitals, with standard quantum numbers l_j , in the pf and $pf g_{9/2}$ shell as neutrons are added to ^{40}Ca . Fig. 1 (a) gives the evolution obtained from phenomenological models: GXPF1 [4], a quasi-global fit of two-body matrix elements (starting from a G -matrix) and of initial SPEs in ^{41}Ca to experimental data; and KB3G [3], which modifies the monopole part of a standard G matrix. Despite different initial SPEs, as neutrons fill the $f_{7/2}$ shell, the repulsive interaction between the $f_{7/2}$ and $p_{3/2}$ neutrons causes a significant gap to develop at $N = 28$, indicative of a shell closure.

In contrast, both NN-only theories in Fig. 1 (b) exhibit minimal repulsion between these orbitals and the gap remains largely unchanged from ^{40}Ca . This is even more evident when the ^{41}Ca SPEs are calculated microscopically at the same third-order level: the NN-only SPEs (based on $V_{\text{low } k}$) are too bound and both $f_{7/2}$ and $p_{3/2}$ orbitals are at -10.8 MeV . Starting from the GXPF1 SPEs in ^{41}Ca , the NN-only results in Fig. 1 (b) depend only weakly on the approach or NN forces used, except for differences for $N > 28$ in the interactions among the p orbitals, mostly $p_{3/2} - p_{3/2}$ (due to more attractive second-order core-polarization and third-order TDA/RPA contributions with $V_{\text{low } k}$, $\Lambda = 2.0\text{ fm}^{-1}$, compared to the G -matrix). This uncertainty remains when 3N forces are

added [see Fig. 1 (c)]. Beyond ^{48}Ca , both NN-only theories predict a shell closure at $N = 34$, which is a major disagreement between the phenomenological models.

The dominant differences between phenomenological forces and NN-only theory can be traced to their two-body monopole components, which determine the average interaction between orbitals [2, 15]. In an operator expansion, the monopole interaction corresponds to the term involving number operators, so that differences are enhanced with N , and the SPE of orbital l_j is effectively shifted by the monopole interaction multiplied by the number of neutrons in orbital l'_j . The interplay of this two-body effect with the initial SPEs largely determines the formation of shell structure.

Next, we include 3N forces among two valence neutrons and one nucleon in the core. In Ref. [6], we have shown that these configurations give rise to repulsive monopole interactions among excess neutrons. This corresponds to the normal-ordered two-body parts of 3N forces, which was found to dominate in coupled-cluster calculations [16] over residual 3N forces (the latter should be weaker because of phase space arguments [17]). For the G -matrix approach, we include FM 3N forces due to Δ excitations, $3\text{N}(\Delta)$, where the parameters are fixed by standard pion- N - Δ couplings [18]. For chiral low-momentum interactions, we take into account chiral 3N forces at N^2LO [19]. These include long-range two-pion-exchange parts c_i (due to Δ and other excitations), plus shorter-range one-pion exchange c_D and 3N contact c_E interactions that have been fit to the ^3H binding energy and the ^4He matter radius [20]. For $V_{\text{low } k}$, we also consider the one- Δ excitation 3N force that corresponds to particular values for the two-pion-exchange part c_i and $c_D = c_E = 0$ [$V_{\text{low } k} + 3\text{N}(\Delta)$] [8]. In the $V_{\text{low } k} + 3\text{N}$ calculations, we also scale all matrix elements by $\hbar\omega \sim A^{-1/3}$.

For all results, full 3N multipole contributions are included to first order [21], although only the monopole part is responsible for the SPE evolution in Fig. 1 (c). Here we see in both microscopic approaches, 3N forces

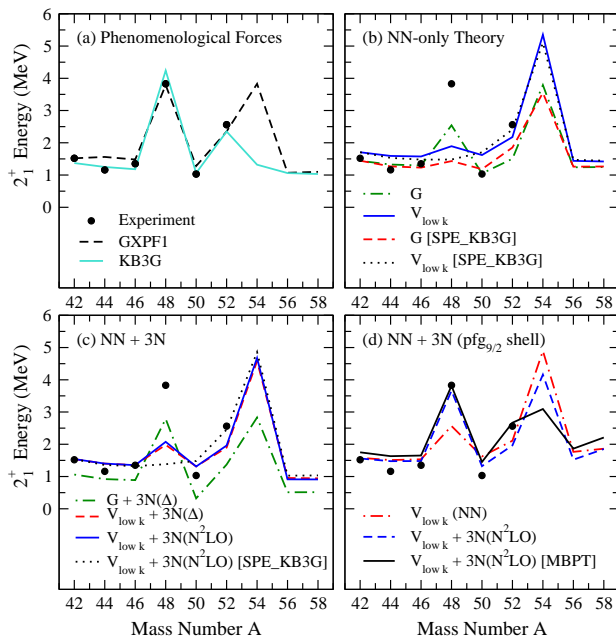


FIG. 2. First 2^+ excitation energies in the even calcium isotopes compared with experiment. (a) Energies obtained from phenomenological models KB3G [3] and GXPF1 [4]. (b) NN-only theory: energies based on a G -matrix and low-momentum interactions $V_{\text{low } k}$ with empirical GXPF1 SPEs in ^{41}Ca , as well as with KB3G values [SPE_KB3G]. (c) Including contributions from 3N forces due to Δ excitations, $3N(\Delta)$, and chiral EFT 3N interactions at $N^2\text{LO}$, $3N(N^2\text{LO})$ [20]. (d) Energies from $V_{\text{low } k}$ and $3N(N^2\text{LO})$ forces in the $pf g_{9/2}$ shell with empirical GXPF1 SPEs and $g_{9/2}$ at -1 MeV in ^{41}Ca , as well as with SPEs in ^{41}Ca calculated consistently in MBPT.

provide repulsive shifts of all single-particle levels, changing the binding energies as shown in Fig. 4. In addition, the repulsion between the $f_{7/2}$ and $p_{3/2}$ orbitals leads to an increased separation at $N = 28$, similarly to the phenomenological forces. Moreover, the gap at $N = 32$ is increased due to the repulsive $p_{3/2} - p_{1/2}$ interaction, while $N = 34$ remains approximately the same.

We take into account many-body correlations by diagonalization in the valence space and plot the first 2^+ energy of the even calcium isotopes in Fig. 2. The excitation energies of the phenomenological models in Fig. 2 (a) show the fit to the high 2^+ energy in ^{48}Ca and hence the doubly-magic nature, and highlight the difference in the prediction of $N = 34$ as a shell closure. In contrast, ^{48}Ca is not reproduced in any calculation based on NN forces in Fig. 2 (b), regardless of starting SPEs, or whether we include the $g_{9/2}$ orbit in Fig. 2 (d).

With 3N forces in Fig. 2 (c), the 2^+ energy in ^{48}Ca is uniformly improved. The pf shell predictions with NN+3N forces are similar with initial GXPF1 SPEs, but still below the experimental value. With KB3G SPEs in ^{41}Ca , the 2^+ energy is significantly lower due to the smaller initial $f_{7/2} - p_{3/2}$ spacing. When the $g_{9/2}$ orbit is included in Fig. 2 (d), the 2^+ energy is obtained very close to experiment. In addition, we find that all microscopic

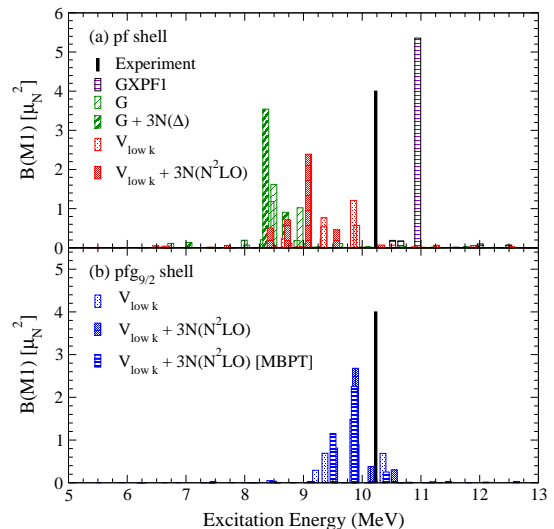


FIG. 3. Magnetic dipole transition rates from the ground state to 1^+ excited states in ^{48}Ca compared with experiment [24]. The $B(M1)$ values are calculated in the pf and $pf g_{9/2}$ shell in panels (a) and (b), respectively, based on NN-only interactions and including 3N forces (spin g factors are quenched by 0.75). The results are labeled as in Fig. 2.

NN-only and NN+3N results at this level yield a high 2^+ energy in ^{54}Ca , and hence a shell closure at $N=34$ (as suggested in Ref. [22]). The similarities of $V_{\text{low } k} + 3N(\Delta)$ and $+3N(N^2\text{LO})$ in Fig. 2 (c) demonstrate that the configurations composed of valence neutrons probe mainly the long-range parts of 3N forces.

To remove the uncertainty in the initial SPEs, we calculate the SPEs in ^{41}Ca by solving the Dyson equation, consistently including one-body contributions to third order in MBPT in the same space as the two-body interactions, and chiral 3N forces between one valence neutron and two core nucleons to first order. In contrast to the failure with NN-only forces, we find in Fig. 1 (d) the pf shell SPEs are generally similar to the empirical ones, and we find the $g_{9/2}$ to initially lie between the $p_{1/2}$ and $f_{5/2}$ orbitals. Our results based on MBPT SPEs and consistent two-valence-neutron interactions are shown in Fig. 2 (d). The agreement with experiment is very promising for a parameter-free calculation based on NN and 3N forces. Furthermore, the high 2^+ in ^{48}Ca , despite a relatively small $f_{7/2} - p_{3/2}$ gap, reflects the possible importance of correlations beyond the pf -shell (in the context of SPEs, see also Ref. [23]). Another challenge for microscopic theories is the prediction of the first excited ($1/2^-$) state in ^{49}Ca , which indicates the size of the $p_{3/2} - p_{1/2}$ gap at $N = 28$. For $V_{\text{low } k} + 3N(N^2\text{LO})$ in both the pf and $pf g_{9/2}$ shell, this energy is ≈ 1.0 MeV compared to the experimental value 2.02 MeV, while the MBPT results yield 1.8 MeV.

We further examine the closed-shell nature of ^{48}Ca in Fig. 3, which shows the magnetic dipole transition rates $B(M1)$ from the 0^+ ground state to 1^+ excited

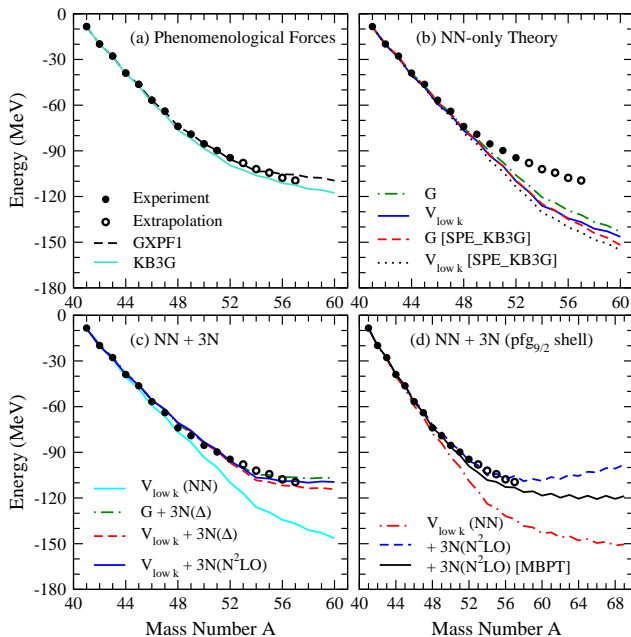


FIG. 4. Ground-state energies of calcium isotopes relative to ^{40}Ca compared with experiment and extrapolated energies from the AME2003 atomic mass evaluation [25]. The panels and results are labeled as in Fig. 2.

states, where the experimental concentration of strength indicates a single-particle transition [24]. With NN-only forces, there is a significant fragmentation of strength, and the energy of the dominant transition is below the observed value. When 3N forces are included, the peak energies are pushed up for all 3N($N^2\text{LO}$) cases. Moreover, the MBPT results predict a clear concentration, in very good agreement with experiment.

Finally, we turn to the ground-state energies in Fig. 4, which have been measured to ^{52}Ca [25] and are known to exist to ^{58}Ca [26]. With phenomenological models, the ground-state energies decrease to $N=34$, then the behavior flattens to $N=40$ due to the weakly-bound $f_{5/2}$ orbital. With NN-only forces in Fig. 4 (b) [as expected from Fig. 1 (b)], all neutron-rich calcium isotopes are overbound. In Fig. 4 (c) and (d) the repulsion due to 3N forces leads to less bound ground-state energies, and all calculations with 3N forces exhibit good agreement with experiment [in Fig. 4 (c) the $V_{\text{low } k} + 3N(N^2\text{LO})$ (KB3G SPE) results would lie on those of $V_{\text{low } k} + 3N(\Delta)$ (GXPF1 SPE)]. The repulsive 3N mechanism, discovered for the oxygen anomaly [6], is therefore robust and general for neutron-rich nuclei. In our best calculation with MBPT SPEs in the $pf_{g9/2}$ shell, the ground-state energies are modestly more bound. Our results with 3N($N^2\text{LO}$) suggest a drip line around ^{60}Ca , which is close to the experimental frontier [26]. As the predicted energies can significantly flatten from $N = 34 - 40$, as is the case in our best MBPT calculation, the inclusion of continuum effects will be very important.

We have presented the first study of the role of 3N

forces for binding energies and evolution of shell structure in medium-mass nuclei, thus linking the 3N forces frontier to the experimental frontier for neutron-rich nuclei. Our results show that 3N forces and an extended valence space are key to explain the $N = 28$ magic number, leading to a high 2^+ excitation energy and a concentrated magnetic dipole transition strength in ^{48}Ca . It is intriguing and promising that the parameter-free MBPT results in the extended valence space reproduce experiment best. Future work will include a detailed comparison to empirically adjusted interactions, where the $pf_{g9/2}$ interactions can also be transformed into pf -shell-only interactions by an Okubo transformation.

This work was supported by the US DOE Grant DE-FC02-07ER41457 (UNEDF SciDAC Collaboration) and DE-FG02-06ER41407 (JUSTIPEN), by grants-in-aid for Scientific Research (A) 20244022 and (C) 22540290, the JSPS Core-to-Core program EFES, and the Alliance Program of the Helmholtz Association (HA216/EMMI). Part of the numerical calculations have been performed on Kraken at NICS, UT/ORNL, and at the JSC, Jülich.

-
- [1] E. Caurier *et al.*, *Rev. Mod. Phys.* **77**, 427 (2005).
 - [2] A. Poves and A. Zuker, *Phys. Rept.* **70**, 235 (1981).
 - [3] A. Poves *et al.*, *Nucl. Phys. A* **694**, 157 (2001).
 - [4] M. T. Honma *et al.*, *Phys. Rev. C* **69**, 034335 (2004).
 - [5] A. P. Zuker, *Phys. Rev. Lett.* **90**, 042502 (2003).
 - [6] T. Otsuka *et al.*, *Phys. Rev. Lett.* **105**, 032501 (2010).
 - [7] J. Fujita and H. Miyazawa, *Prog. Theor. Phys.* **17**, 360 (1957); Proceedings of the International Symposium “New Facet of Three Nucleon Force - 50 Years of Fujita Miyazawa Three Nucleon Force (FM50)”, Eds. H. Sakai *et al.* (AIP, 2008).
 - [8] E. Epelbaum *et al.*, *Rev. Mod. Phys.* **81**, 1773 (2009).
 - [9] P. Navrátil *et al.*, *J. Phys. G* **36** 083101 (2009).
 - [10] S. K. Bogner *et al.*, *Nucl. Phys. A* **784**, 79 (2007); *Prog. Part. Nucl. Phys.* **65** 94 (2010).
 - [11] D. R. Entem and R. Machleidt, *Phys. Rev. C* **68**, 041001(R) (2003).
 - [12] T. T. S. Kuo and E. Osnes, *Springer Lecture Notes of Physics*, 1990, Vol. 364, p. 1.
 - [13] M. Hjorth-Jensen *et al.*, *Phys. Rept.* **261**, 125 (1995).
 - [14] G. Hagen *et al.*, *Phys. Rev. C* **82**, 034330 (2010).
 - [15] T. Otsuka *et al.*, *Phys. Rev. Lett.* **104**, 012501 (2010).
 - [16] G. Hagen *et al.*, *Phys. Rev. C* **76**, 034302 (2007).
 - [17] B. Friman and A. Schwenk, in *From Nuclei to Stars: Festschrift in Honor of Gerald E. Brown*, Ed. S. Lee (World Scientific, 2011) arXiv:1101.4858.
 - [18] A. M. Green, *Rep. Prog. Phys.* **39**, 1109 (1976).
 - [19] U. von Kolck, *Phys. Rev. C* **49**, 2932 (1994); E. Epelbaum *et al.*, *Phys. Rev. C* **66**, 064001 (2002).
 - [20] S. K. Bogner *et al.*, arXiv:0903.3366. We use the 3N couplings fit to the ^3H binding energy and the ^4He radius for the smooth-cutoff $V_{\text{low } k}$ with $\Lambda = \Lambda_{3N} = 2.0 \text{ fm}^{-1}$.
 - [21] The first-order 3N contribution also dominates the neutron matter energy, see K. Hebeler and A. Schwenk, *Phys. Rev. C* **82**, 014314 (2010).

- [22] T. Otsuka *et al.*, Phys. Rev. Lett **87**, 082502 (2001).
- [23] T. Duguet and G. Hagen, Phys. Rev. C **85**, 034330 (2012).
- [24] P. von Neumann-Cosel *et al.*, Phys. Lett. B **443**, 1 (1998).
- [25] G. Audi *et al.*, Nucl. Phys. A **729**, 337 (2003).
- [26] M. Langevin *et al.*, Phys. Lett. B **130**, 251 (1983); M. Bernas *et al.*, Phys. Lett. B **415**, 111 (1997); O. B. Tarasov *et al.*, Phys. Rev. C **80**, 034609 (2009).